

In-situ resistive left-tilt selective laser sintering for high-conductivity Cu matrix



K. Cui^a, W. Jiang^a, Li Jiang^{a*}, Li Hong^a, C. Zhang^a, G. Li^a, F. Li^b, S. Wang^c, K. Lis Ess^d, Li Lu^a, J. Guo^a, T. P. Jijs^e

^aGemological Institute, China University of Geosciences, Wuhan 430074, PR China
^bHubei Gem and Jewelry Engineering Technology Research Center, Wuhan 430074, PR China
^cSchool of Materials Science and Engineering, Huazhong University of Science and Technology, Wuhan 430074, PR China
^dMechanical Engineering, University of Birmingham, Birmingham B15 2TT, UK
^eSchool of Electrical and Electronic Engineering, Huazhong University of Science and Technology, Wuhan 430074, PR China
^fWMG, Materials Engineering Centre, University of Warwick, CV4 7AL Coventry, UK

ARTICLE INFO

Keywords:
Ternary system
Composite synthesis
Selective laser sintering
Ceramic matrix
Electromagnetic shielding

ABSTRACT

Currently, ternary system (3DG) fabrication still greatly depends on the traditional casting process. However, the selective laser sintering (SLM) technique for ternary system (3D) composites is still in its infancy. This work presents a novel in-situ resistive (CVD) ceramic matrix composite (CVC) for 3DG composites. A ceramic matrix composite (CVC) is fabricated by SLM for the selective laser sintering process. The tensile strength of 3DG composites is significantly improved. The density of the 3DG composites is increased by 88% and 27% compared to the matrix material. The electromagnetic interference shielding efficiency (SE) is improved by 47.8 dB to 2.7 GHz and 32.3 dB to 2–18 GHz. This study illustrates the feasibility of the selective laser sintering process for ternary systems.

1. Introduction

Generally, resistive of sp^2 carbon materials, such as graphite and carbon fiber, have a high conductivity (2630 2^{-1}) [1], and high thermal stability (2 10^5 2^{-1} V $^{-1}$ s $^{-1}$) [2]. However, the π - π interaction between the adjacent (2D) sheets of carbon materials is weak, leading to a poor thermal stability, which is not suitable for high-temperature applications [3]. After the first successful synthesis of carbon fiber [4], the 3DG composites are widely used in many fields. The 3DG composites have a high conductivity (~99.7%), high strength (~0.6 10^8 N/m 2) [5] and excellent thermal stability, fast thermal conductivity [6].

(2DG), thermal stability [5], system [6,7], synthesis [4], and thermal stability (EMI shielding) [8] are very important factors in 3DG composites. However, the fabrication of ternary systems still faces many challenges. For example, the synthesis of ternary systems is still in its infancy [9], and the thermal stability [10], synthesis [11], and properties [12] are not fully understood. Therefore, the synthesis of ternary systems still faces many challenges. For example, the synthesis of ternary systems is still in its infancy [9], and the thermal stability [10], synthesis [11], and properties [12] are not fully understood. Therefore, the synthesis of ternary systems still faces many challenges.

* Corresponding author. E-mail address: jiangli@cgic.cug.edu.cn (L. Jiang).
E-mail address: yji@u.warwick.ac.uk (T. P. Jijs).

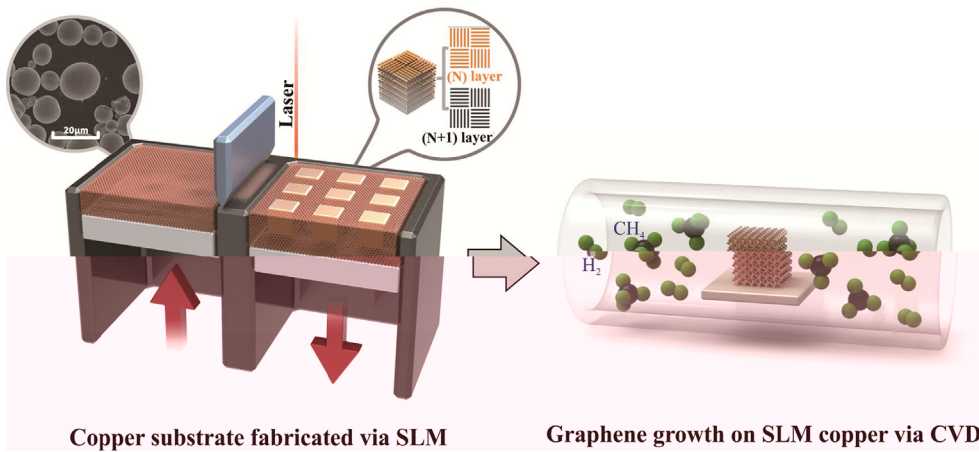


Fig. 1. Illustration of the 3DG/C process: (a) SLM fabrication of copper substrate; (b) in-situ CVD growth of graphene on SLM copper.

ASTM B193-2002 (2003) and ASTM E1461-2013 (2013) for tensile and compressive strength, respectively. The test specimens were prepared according to the standard of LFA (Laser Flash Analysis, Netzsch LFA457, Germany). The test specimens were SENTERRA, B (Germany) standard type 3DG/C specimens with a diameter of 514 μm . The test specimens (S11-S21) were tested at a frequency of 2–18 GHz. The test specimens were tested using a VNA (Vector Network Analyzer, PNA-N5244A, Agilent) with a resolution bandwidth of 200 Hz. The test specimens were tested at a distance of 2–18 GHz. The test specimens were tested using a SE (Secondary Electron) detector, SE detector type E-2-5 in the SEM.

3. Results and discussion

3.1. Formation of SLM copper

3.1.1. SLM manufacturing of copper under different line energy densities

The test specimens were prepared under different line energy densities. The test specimens were prepared under different line energy densities.

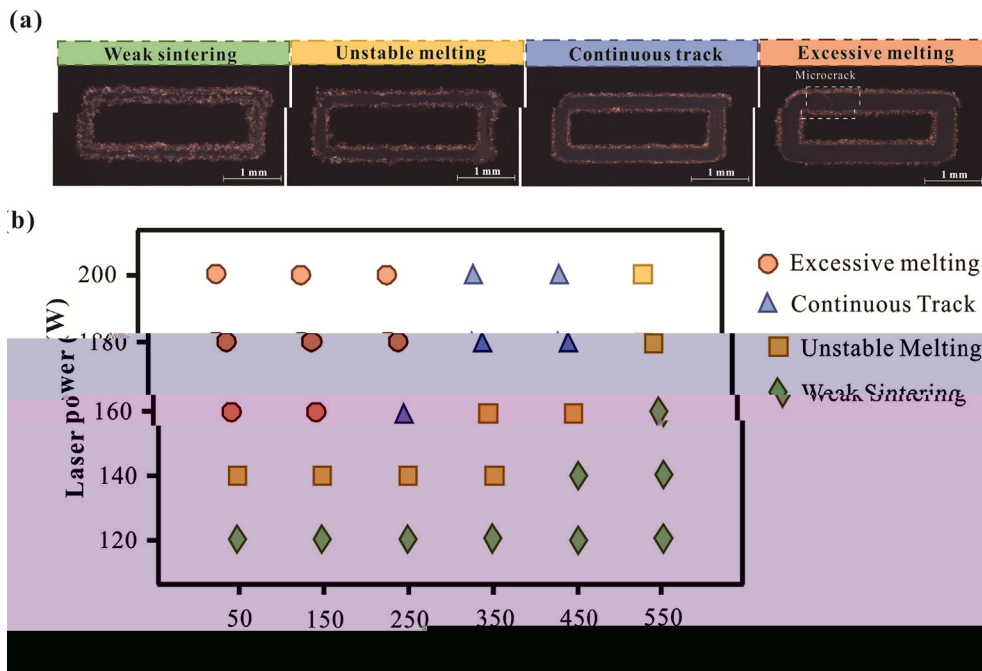


Fig. 2. (a) Typical SEM images of SLM copper tracks under different melting conditions: (a) Weak sintering; (b) Unstable melting; (c) Continuous track; (d) Excessive melting. (b) Laser power vs. line energy density for different melting conditions.

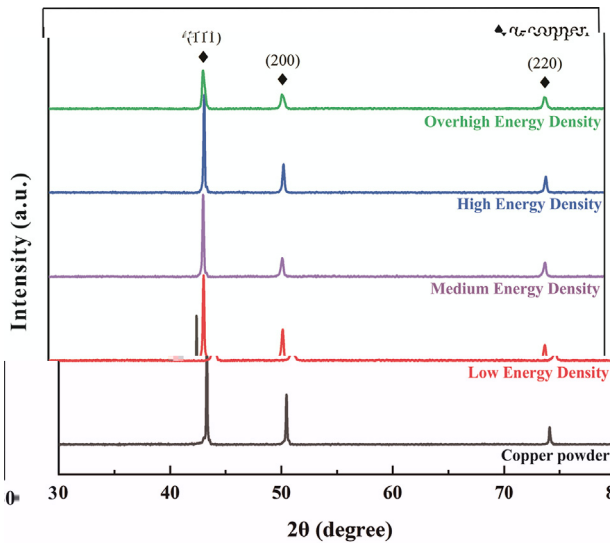


Fig. 3. XRD patterns of copper powder at different energy densities. (For interpretation of the references to colour in this figure legend, the reader is referred to the web version of this article.)

3.1.2. Formation of anisotropic microstructure under different volumetric energy density

The α -copper phase is the main phase in the SLM process. The XRD patterns of the copper powder at different energy densities are shown in Fig. 3. The main peaks are indexed to the (111), (200) and (220) planes. The intensity of the (111) peak is the highest, which indicates that the copper powder has a strong preferred orientation along the (111) plane. The intensity of the (111) peak increases with increasing energy density, indicating that the preferred orientation becomes stronger. This is due to the fact that the laser energy density affects the grain growth and orientation of the copper powder during the SLM process. At higher energy densities, the laser energy is more concentrated, leading to higher temperatures and faster grain growth, which results in a more pronounced preferred orientation.

The XRD patterns of the copper powder at different energy densities are shown in Fig. 3. The main peaks are indexed to the (111), (200) and (220) planes. The intensity of the (111) peak is the highest, which indicates that the copper powder has a strong preferred orientation along the (111) plane. The intensity of the (111) peak increases with increasing energy density, indicating that the preferred orientation becomes stronger. This is due to the fact that the laser energy density affects the grain growth and orientation of the copper powder during the SLM process. At higher energy densities, the laser energy is more concentrated, leading to higher temperatures and faster grain growth, which results in a more pronounced preferred orientation.

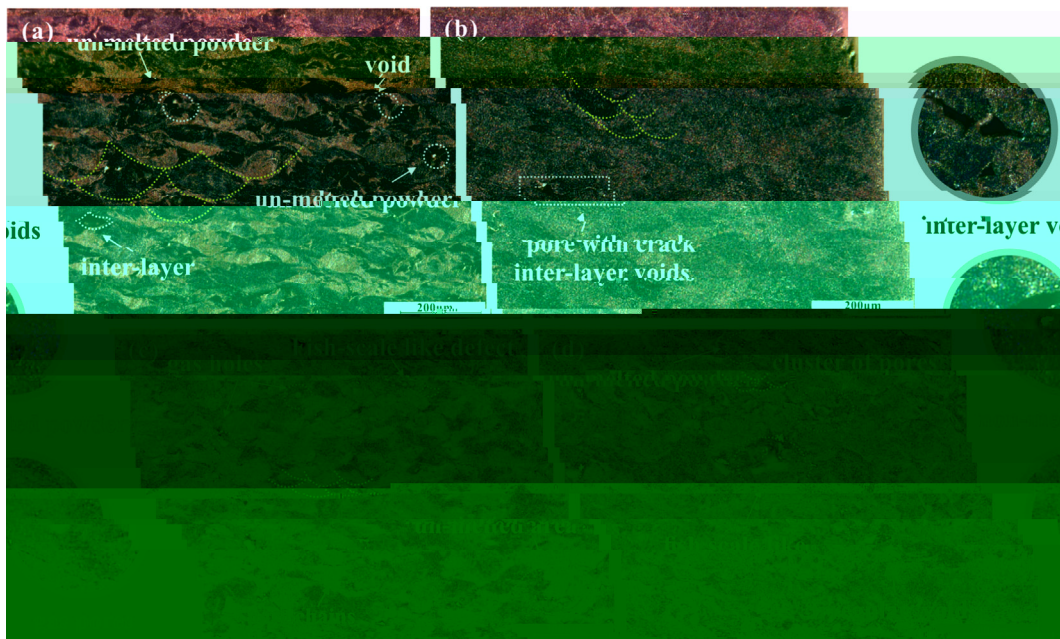


Fig. 4. Optical micrographs of copper powder at different energy densities: (a) 3000 J/cm³, (b) 857 J/cm³, (c) 285 J/cm³, (d) 128 J/cm³. (For interpretation of the references to colour in this figure legend, the reader is referred to the web version of this article.)

t i t e t e t s e i e i e t.

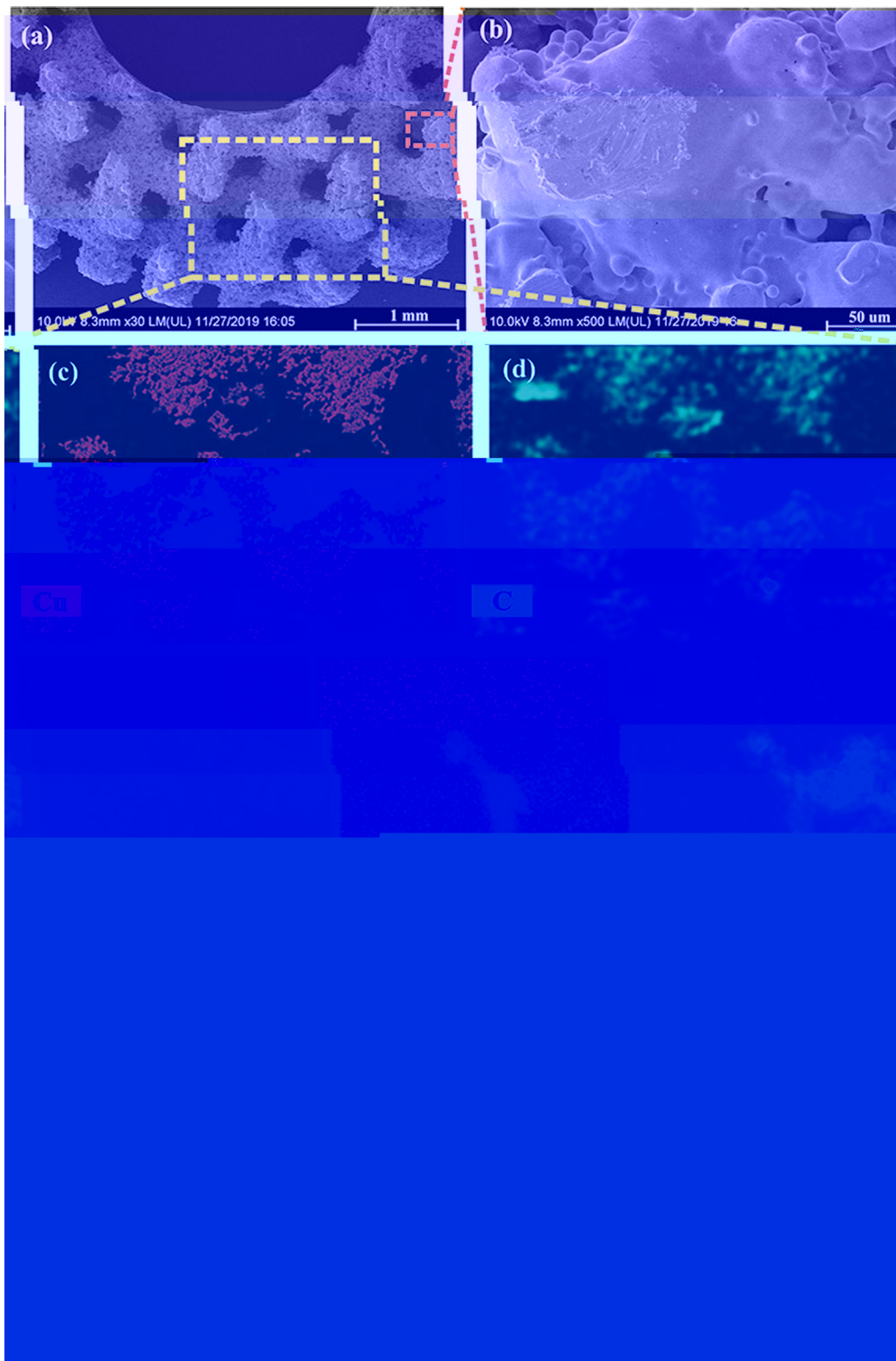


Fig. 8. (a) SEM image of 3DG/C porous scaffold; EDS image of (b) C; (c) O; (d) EDS image of SEM image, EDS image of (f) C; (g) O; (h) EDS image of SEM image of OM; (i) Results of EDS image of porous scaffold; (j) Results of EDS image of porous scaffold.

It is the density of foams. With respect to the density of foams, the ratio of I_D/I_G is from 0.71 to 0.93, indicating the presence of foams. As a result, the porous scaffold (prepared at 1000 °C, flow rate of CH_4 is 30 sccm, reaction time of 20 min) is synthesized from 3DG/C porous scaffold.

3.4. Thermal property and EMI shielding effectiveness of 3DG/Cu porous scaffolds

The thermal stability of porous scaffolds is an important property of porous scaffolds, and the porous scaffolds prepared at 1000 °C for 20 min have a weight loss of 14.8% at 1000 °C.

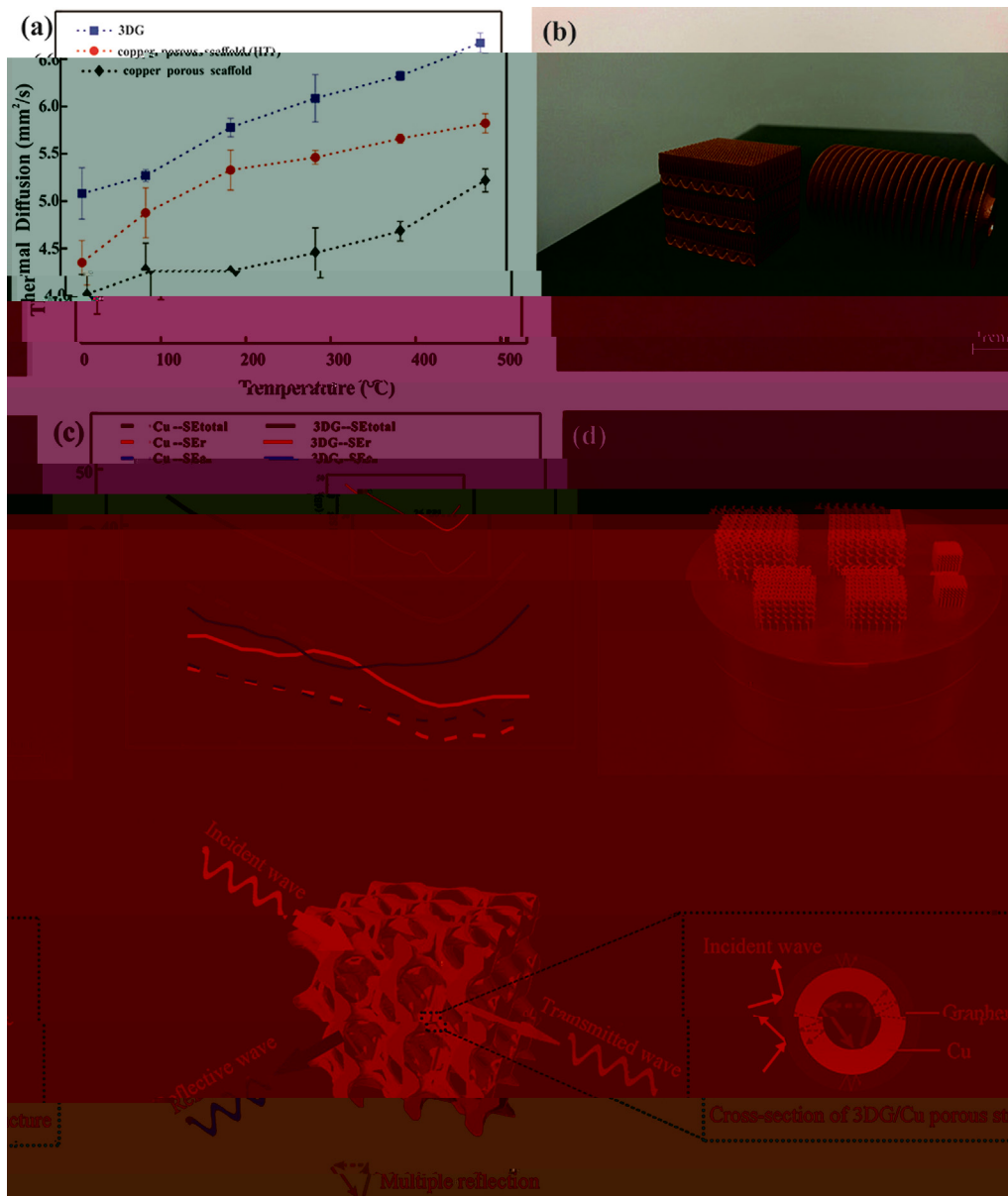


Fig. 9. Performance of 3DG/C porous scaffold: (a) thermal diffusion; (b) SLM porous structure; (c) EMI SE; (d) Cross-section of porous scaffold. (Inset: Schematic of 3DG/C porous structure EMI. (For interpretation of the references to colour in this figure legend, the reader is referred to the web version of this article.)

Table 1

Comparison of the EMI shielding performance of porous structures with different porous materials and porous structures. (For interpretation of the references to colour in this figure legend, the reader is referred to the web version of this article.)

Coating materials	Substrate	Method	Maximum shielding efficiency (dB)	Improvement of thermal property (%)	Ref
G	PPS	Infiltration + freeze-drying + sintering	37	-	50]
G	PS	Hydrothermal synthesis + sintering	29.3	-	56]
G	PMMA	Sol-gel + freeze-drying + sintering	19	-	57]
C /G	/C	Sintering + freeze-drying	-	8.5	58]
G	Ni	Freeze-drying + CVD	-	554	59]
G	C-Ni	Electrodeposition + freeze-drying	20	-	60]
G	C	Precipitation + CVD	-	2.4	61]
G	PPS	Freeze-drying + sintering	47	6.3	62]
G	C	CVD + SLM	47.8	27	This work

Note: PPS (poly (styrene)-PPMA, polystyrene-PS.

Declaration of Competing Interest

The authors declare that they have no competing interests.

Acknowledgement

The authors thank the following for their financial support: National Natural Science Foundation of China (Nos. 51671091, No. 51902295, No. 51675496). The authors thank the following for their support: Faculty of Resources Environment and Ecology, University of Georgia (USA) (No. (No. CUG170677) H. Li; P. Li; N. Li; S. Li; F. Li; T. Li (No. 2019 CFB264).

Appendix A. Supplementary data

Supplementary data for this article is available at <https://doi.org/10.1016/j.jes.2020.105904>.

References

- 1] B. J. R. G., N. Li, M. T. P. S. Y. K., M. Li, S. G. ... : s. t. i. l. | t. f. e. f. e. ...
- 2] B. J. R. G., A. G. S. S., B. W. C., L. H. L., T. ... D., M. F. E., t. l. S. ...
- 3] Li, H., C. S. M., P. H. J., P. O., S. T. J. G., t. l. I. s. i. t. ...
- 4] K. M., K. J., J. B. C., K. J. H., A. J. H. G. ... s. t. i. l. | s. i. l. | ...
- 5] P. C., M. H. M., T. M., L. D. P. ... t. l. I. s. i. t. ...
- 6] Li, J., W. C., L. L., J. S. H., W. G., L., t. l. F. l. | | C- G. l. f. e. ...
- 7] H. Q., L. S. W., C. L. H., J. S. H., H. Q. S. ... t. l. I. s. i. t. ...
- 8] D. L. S. T. M., S. i. l. | P., D. i. s. y. t. P., K. t. J., K. M., A. i. s. e. T., t. l. 3D ...
- 9] Q. L., L. L., T. ... i. s. i. l. | P. e. s. ... t. l. I. s. i. t. ...
- 10] D. H., L. S. P., N. W. J. G. 3D ... t. l. I. s. i. t. ...
- 11] Li, L., W. S., C. Q., H. M. K., H. L., D. W., t. l. S. l. f. s. s. l. y. e. - s. l. | ...
- 12] Li, J., P., L. C., R. G., N. T. S. D., t. l. G. ... t. l. I. s. i. t. ...
- 13] J. S. H., A. J. S. G. A. L. e. - s. i. t. y. e. ... t. l. I. s. i. t. ...
- 14] I. T., S. K., K. S. M., T. S. T., T. I. K., t. l. T. ... t. l. I. s. i. t. ...
- 15] S. K., D. i. t. e. N., M. J. C., V. s. i. j. i. N., E. J. T. ... t. l. I. s. i. t. ...
- 16] C. H., S. L. M., S. W. H., L. G. H., Q., t. l. P. ... t. l. I. s. i. t. ...
- 17] K. S. H., G. M., J. S. L., H. J. W. C., C. M. U. ... t. l. I. s. i. t. ...
- 18] S. Q., F., L. W., L. H., L., t. l. C. ... t. l. I. s. i. t. ...
- 19] G. C., L. T. H., D. W., t. l. T. ... t. l. I. s. i. t. ...
- 20] C. C., H. B., N. J., C. S., L. F., t. l. 3D ... t. l. I. s. i. t. ...
- 21] St. Ćić J., B. Žić D. T. f. t. e. f. N. B. i. t. i. s. f. e. ... t. l. I. s. i. t. ...

- 22] R. D. C., H. B., L. J., L. S. J., J. W., R., t. l. M. i. e. s. t. t. ... t. l. I. s. i. t. ...
- 23] Li, C. W., A. J. K., S. N. J., D., t. l. L. - s. y. t. s. i. s. e. f. l. - l. i. t. y. ...
- 24] C. P., R. W. C., G. L. B., L. B. L., P. S. E., C. H. M. T. ... t. l. I. s. i. t. ...
- 25] J. S. D., D. S. S., G. S. S., L. K. T. J. P., H. J. V., V. S. J. K. ... t. l. I. s. i. t. ...
- 26] W. H. E., L. L., T. D., C. I. Q., F., t. l. E. f. f. e. t. s. | t. i. l. s. | t. i. ...
- 27] G. D. D., M. S. W., W. S. K., P. R. L. S. ... t. l. I. s. i. t. ...
- 28] Li, E., T. S. S., C. S. L., F. e. t. e. A. E. f. f. e. t. s. | t. i. l. s. | t. i. (SLM) ...
- 29] S. W. S., W. L. J., W. P. C., t. l. F. e. l. i. f. t. y. s. i. s. f. e. ...
- 30] Li, M. S., D. W., S. C. I. s. t. i. t. i. e. t. e. s. t. t. ... t. l. I. s. i. t. ...
- 31] L. C. L. A., M. S. S. S., T. i. M., A. t. e. R. C., W. i. t. S. P. J., L. P. D. T. ...
- 32] T. K., T. W. Q., T. J. D. S. S. M., M. J. D., t. l. R. J. ... t. l. I. s. i. t. ...
- 33] K. H. T., P. L. N. H., T. S. B., C. K. G. e. t. y. ... t. l. I. s. i. t. ...
- 34] R. H. K., K. T. N. V., G. H. S., T. L. S., T. L. S. B. E. M. i. e. s. t. t. s. ...
- 35] T. K., T. J. V. S. G., P. I. Q., G., t. l. A. ... t. l. I. s. i. t. ...
- 36] R. D. A., M. L. E., M. T. H., t. l. N. e. | i. t. t. - i. e. s. t. t. | ...
- 37] W. H. E. f. f. e. t. y. s. t. | l. e. i. t. t. s. e. t. | - i. s. e. t. y. e. f. s. | t. i. l. s. | t. C - 2.4N1 - 0.7S1 | l. e. J. A. l. l. e. y. C. ...
- 38] K. S. W. l. i. t. | l. y. S. E. E. t. i. e. 2003;23:309-48.
- 39] L. G. S. G. s. t. J. f. f. y. R., G. S. i. N. t. P. E. i. t. | | C (111). N. e. ...
- 40] Li, S. C. I. W. W., C. e. l. L. i. R. e. f. R. e. y. S. E. e. l. i. e. f. ... t. l. I. s. i. t. ...
- 41] W. C., W. H., L. S. Q., L. A. S. | l. e. y. - f. ... t. l. I. s. i. t. ...
- 42] F. A. C., M. y. J. C., S. V., C. S. i. C., L. i. M., M. F., t. l. R. ...
- 43] S. G., J. S. H., F. P. C., H. Q. F. l. | | f. t. e. y. t. | ... t. l. I. s. i. t. ...
- 44] J. K., E. H., J. C. J., D. i. F. l. i. e. | t. e. t. i. t. f. ... t. l. I. s. i. t. ...
- 45] R. J. K., M. J. D. P., A. S. C., M. S., S. e. j. K. E. | l. t. E. M. i. s. i. l. i. ...
- 46] S. B., L. i. W., W. C. S. i. | - e. t. e. y. f. e. s. i. t. ... t. l. I. s. i. t. ...
- 47] L. N., H., D. F., H., L. i., G. W.

Mt 2019;34(5):489–98.

53] W B, C M, L M. R. *Composites: Part B*. 2014;26:3484–9.

54] C H, W S, J J, C J, J. *Synthetic modification of Fe₃O₄ nanoparticles for poly(vinylidene fluoride) nanocomposites*. *Compos Part A* 2019;121:139–48.

55] W L, J, Q. *Tensile strength of MWCNTs reinforced polyethylene terephthalate-MWCNTs nanocomposites*. *J Mater Sci: Mater Electron* 2015;26(3):1895–9.

56] D G, P G, H P, Q F, M B, M. *ML Efficiently detects and classifies malicious URLs*. *ACS Appl Mater Electron* 2012;22:18772–4.

57] H B, Q, W G, H, T. *Thermal stability of polyethylene glycol nanofiber reinforced polyethylene glycol*. *ACS Appl Mater Electron* 2011;3:918–24.

58] S A, U N, T V. *Tensile strength of polyethylene glycol nanofiber reinforced polyethylene glycol*. *Mater Res* 2016. <https://doi.org/10.1051/mater/2016021>.

59] P M, J H, R S, S L. *Tensile strength of polyethylene glycol nanofiber reinforced polyethylene glycol*. *Nanotechnol* 2012;12:2959–64.

60] J K, H H, D P. *Preparation of polyethylene glycol–Ni alloy nanofiber reinforced polyethylene glycol nanocomposites*. *Mater Lett* 2017;122:244–7.

61] R H, L S, B S, K T, L D, L H, J. *Tensile strength of polyethylene glycol nanofiber reinforced polyethylene glycol*. *SIR* 2015. <https://doi.org/10.1038/s12710-015-0127-1>.

62] T, F S, L G, Q, L G, R K, J. *Synthesis and characterization of polyethylene glycol nanofiber reinforced polyethylene glycol nanocomposites*. *3D Nanotechnol* 2020. <https://doi.org/10.1016/j.3dnano.2019.105670>.

63] R D, M L, M E, H D, M J, M B, J. *Nanofiber reinforced polyethylene glycol nanocomposites*. *ACS Appl Mater Electron* 2011;59(10):4088–99.

64] E S, L K, S V, M C. *Tensile strength of polyethylene glycol nanofiber reinforced polyethylene glycol*. *J Mater Electron* 1973;1(1):10–38.